

Characterizing the CCD Cameras for Fan Mountain Observatory

May 7, 2003

David McDavid, Heather Welch¹, and Kiriaki Xilouris

Department of Astronomy, University of Virginia, PO Box 3818, Charlottesville VA 22903

`dam3ma@virginia.edu, hew9e@virginia.edu, kx8u@virginia.edu`

ABSTRACT

We describe laboratory measurements of the basic operating parameters of two SDSU CCD cameras with a SITE2048 arrays. The resulting calibration data are in use in research projects with the 1m telescope at the University of Virginia Fan Mountain Observatory.

Subject headings: instrumentation: detectors—methods: laboratory— techniques: image processing—techniques: photometric

1. Photon Transfer Curve Method

Accurate quantitative estimates of the characteristics of a CCD camera system are necessary for the reduction of images to standard photometric data. The gain, readout noise, full well capacity, and linearity are most commonly measured by analysis of the photon transfer curve, which is explained in theoretical detail by Janesick (2001). Here we give a derivation of the simplified method we used in practice.

The gain K is the constant for conversion of the camera output signal in analog-to-digital units $S(\text{ADU})$ to the actual physical number of electrons $N(e^-)$ generated by incident photons interacting with the CCD. It has units of electrons per ADU ($e^- \text{ADU}^{-1}$) and is defined by

$$N = KS. \tag{1}$$

Since N is directly proportional to S , their errors are also directly proportional by the same constant:

$$\sigma_N = K\sigma_S. \tag{2}$$

¹Heather Welch received undergraduate academic credit for this project as part of an independent study course during the Spring 2003 Semester.

Assuming that electrons are produced by the CCD in direct proportion to the number of incident photons, N should obey photon counting statistics, so that

$$\sigma_N = \sqrt{N}, \quad (3)$$

which gives

$$\sqrt{N} = K\sigma_S. \quad (4)$$

Using equation (1) for N ,

$$\sqrt{KS} = K\sigma_S, \quad (5)$$

and we have the equation of the photon transfer curve:

$$\sigma_S^2 = \frac{1}{K}S, \quad (6)$$

which says that a graph of the variance of S as a function of S should be a straight line with a slope equal to the reciprocal of the gain.

2. Laboratory Procedure

The cameras we tested are based on the SITE SI-424A CCD chip, which has 4 output amplifiers. The GENII camera has SDSU GENII control system electronics (Leach & Low 2000; Leach, Beale, & Eriksen 1998), allowing each amplifier to be used individually with any combination of 4 different gain settings and 2 different data conversion rates to read out the full array or any subarray under the **Voodoo V1.7** control software. **Voodoo V1.7** is designed to communicate with the controller over a PCI bus interface. The GENI camera has SDSU GENI control system electronics, an earlier version with single-amplifier readout, no subarray capability, and 2 different gain settings. It runs under the **ccdtool** control software, which communicates with the controller over an SBUS interface.

For the GENII camera calibration, unbinned 16-bit full frames of 2400 columns and 2048 rows including an overscan section were taken for each amplifier at gain setting 1.0 in slow conversion mode with MPP disabled and temperature regulated to -110°C . Each data set consisted of a pair of 0s bias images, one 600s dark image, and 5 to 7 pairs of unfocused images in diffuse light in a laboratory room with the direct unlensed CCD covered by 16 layers of laser printer paper and shuttered for times ranging from 10s to 70s to cover the full range from low level exposure to near

saturation. We chose the same relatively uniform 100×100 pixel section of each image in a data set for each individual determination of characteristic parameters.

For the GENI camera calibration, data were acquired in much the same way, except the camera was mounted on the 1m telescope at Fan Mountain Observatory. Normal procedures for taking dome flats were followed, using a white painted section on the inside of the dome illuminated by dim lamps.

3. Data Reduction & Analysis

We used IRAF¹ (Tody 1993) to extract the data for plotting photon transfer curves. The camera control software writes image files in FITS format (Hanisch et al. 1999) using the keyword BITPIX=16, which specifies that the pixel values are represented in 16-bit twos-complement binary integer format. Since the raw pixel data written to the files are the output of a 16-bit A/D converter, they are binary integers in the interval $[0, 65535]$. When these bit patterns are interpreted as 16-bit twos-complement binary integers, the interval $[0, 32767]$ is unchanged, but the interval $[32768, 65535]$ is mapped into the interval $[-32768, -1]$. In order to restore the original image data it is therefore necessary to add 65536 to all pixel values in the interval $[-32768, -1]$, which is readily done with IRAF. Changes are being written into both camera control programs to eliminate this inconvenience without increasing the file size.

The exposed frames and the dark frames were bias-subtracted using the overscan section, but the bias frames were not. The image sections selected for analysis were then trimmed out of all frames. Difference image sections were constructed from each pair of the exposed image sections, and complete sets of statistics were computed for all sections. We used the difference sections to evaluate the signal variance in order to eliminate the contribution of flat-field variations, taking half the variance of each difference section since the individual variances add when the frames are combined. Taking the mean of each pair of exposed image sections as the signal, we plotted the photon transfer curve, then calculated the gain from a linear least squares fit inversely weighted by the variance. We took the standard deviation of a bias frame section as the readout noise and converted it to electrons using the derived gain. A lower limit to the full well capacity was found by converting the highest signal data value lying on the best fit straight line to electrons. Data points which were clearly beyond the saturation limit were eliminated from the fits. The dark current in units of $(e^{-1} s^{-1})$ was calculated by dividing the mean signal in the dark image section minus the readout noise by the dark integration time and applying the gain constant.

We made two tests of linearity: variance vs. signal (the photon transfer curve) and signal vs. exposure time. The rms deviations of linear least squares fits were calculated as estimates of the

¹IRAF is distributed by the National Optical Astronomy Observatories, which are operated by the Association of Universities for Research in Astronomy, Inc., under cooperative agreement with the National Science Foundation.

deviations from linearity for both cases, ignoring points which were clearly beyond the full well capacity.

4. Conclusions

The characteristic parameters we measured for the GENII camera are summarized in Table 1. Figures 1–4 show the graphical analysis for the 4 output amplifiers of the CCD.

Amplifier A appears to have a readout noise problem, as well as the highest nonlinearity. Amplifier B would be a good choice for bright objects with its large full well, while Amplifier C would probably be better for faint objects since it produces more output signal per photon. Amplifier D shows a severely low threshold for saturation, although its readout noise and linearity at low light levels are the best of the set.

These results should be considered preliminary, since we do not yet have enough repeated measurements to estimate their uncertainties. Analyzing different image sections of the existing data may be the easiest way to increase our confidence by checking the repeatability of the derived parameters.

Results for the GENI camera are summarized in Table 2, with the graphical analysis shown in Figures 5–10. In this case we analyzed three different image sections for each gain setting and calculated the mean and standard deviation of each parameter in order to estimate the precision of our results. The apparent uniformity of the HIGH gain data is misleading; in practice we had to work much harder to obtain consistent sets of frames at this setting than we did for the LOW gain measurements.

REFERENCES

- Hanisch, R.J. et al. 1999, Definition of the Flexible Image Transport System (FITS), Standard NOST 100-2.0, NASA/Science Office of Standards and Technology
- Janesick, J.R. 2001, Scientific Charge-Coupled Devices, 95 (Bellingham: SPIE)
- Leach, R.W. & Low, F.J. 2000, in Optical and IR Telescope Instrumentation and Detectors, Proc. SPIE, Vol. 4008, eds. M. Iye & A.F. Moorwood, 337
- Leach, R.W., Beale, F.L., & Eriksen, J.E. 1998, in Optical Astronomical Instrumentation, Proc. SPIE, Vol. 3355, ed. S. D’Odorico, 512
- Tody, D. 1993, in Astronomical Data Analysis Software and Systems II, A.S.P. Conference Ser., Vol. 52, eds. R.J. Hanish, R.J.V. Brissenden, & J. Barnes, 173

Table 1. Summary of GENII Camera Characteristics

| Amplifier | Gain Setting | Bias (ADU) | Fitted Gain ($e^- \text{ ADU}^{-1}$) | Full Well (e^-) | Readout Noise (e^-) | Dark Current ($e^- \times 10^{-2} \text{ s}^{-1}$) | RMS Nonlinearity of Variance (%) | RMS Nonlinearity of Exposure (%) |
|-----------|--------------|------------|--|---------------------|-------------------------|--|----------------------------------|----------------------------------|
| A | 1.0 | 1319 | 2.94 | > 174,000 | 26.5 | 3.5 | 1.79 | 0.84 |
| B | 1.0 | 1321 | 3.63 | > 213,000 | 8.8 | 6.0 | 0.73 | 0.93 |
| C | 1.0 | 1285 | 2.92 | > 179,000 | 8.3 | 6.7 | 0.99 | 0.78 |
| D | 1.0 | 1253 | 3.30 | > 125,000 | 5.6 | 0.05 | 0.20 | 0.28 |

Table 2. Summary of GENI Camera Characteristics

| Gain Setting | Bias (ADU) | Fitted Gain ($e^- \text{ ADU}^{-1}$) | Full Well (e^-) | Readout Noise (e^-) | Dark Current ($e^- \times 10^{-2} \text{ s}^{-1}$) | RMS Nonlinearity of Variance (%) | RMS Nonlinearity of Exposure (%) |
|--------------|------------|--|---------------------|-------------------------|--|----------------------------------|----------------------------------|
| LOW | 743±1 | 3.84±0.11 | > 180,000 ± 30,000 | 8.9±0.2 | ~ 0.1 | 1.60±0.41 | 3.80±0.03 |
| HIGH | 6369±3 | 2.06±0.01 | > 103,000 ± 500 | 16.9±0.1 | ~ 0.1 | 1.14±0.24 | 1.66±0.33 |

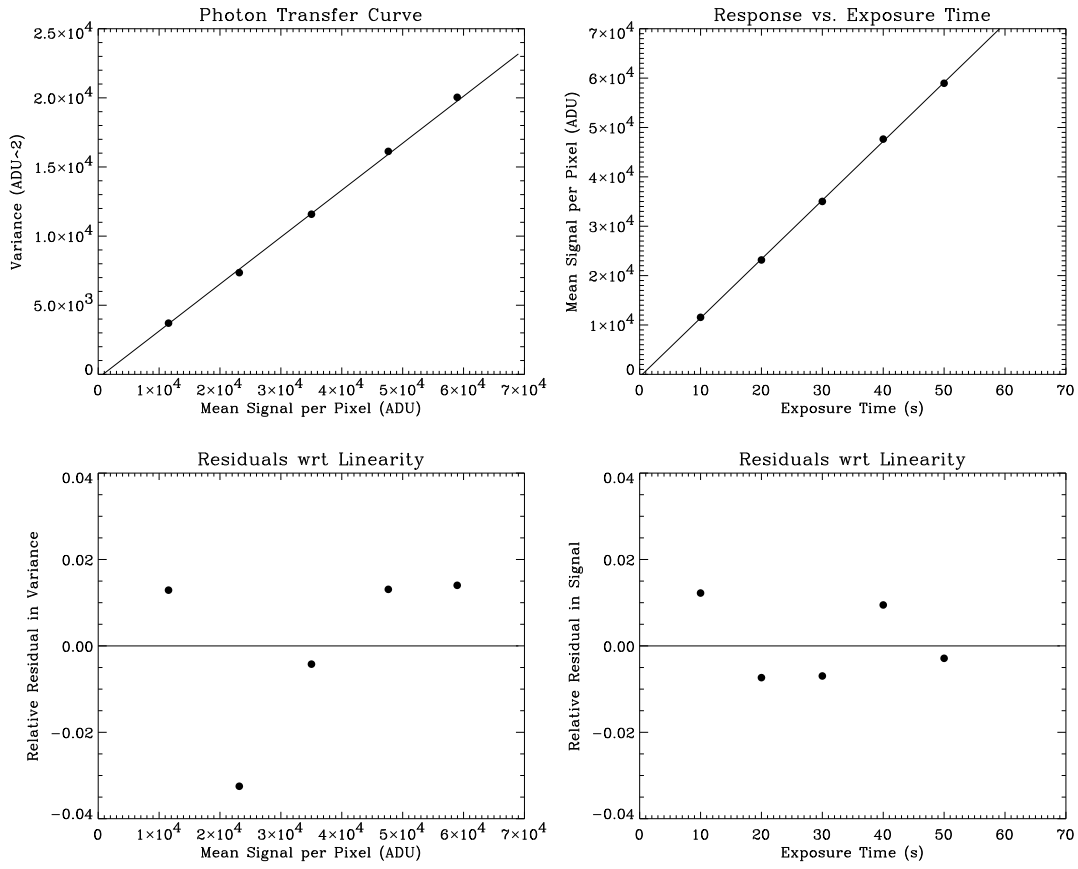


Fig. 1.— Performance curves for the GENII Camera, Amplifier A, Gain Setting 1.0.

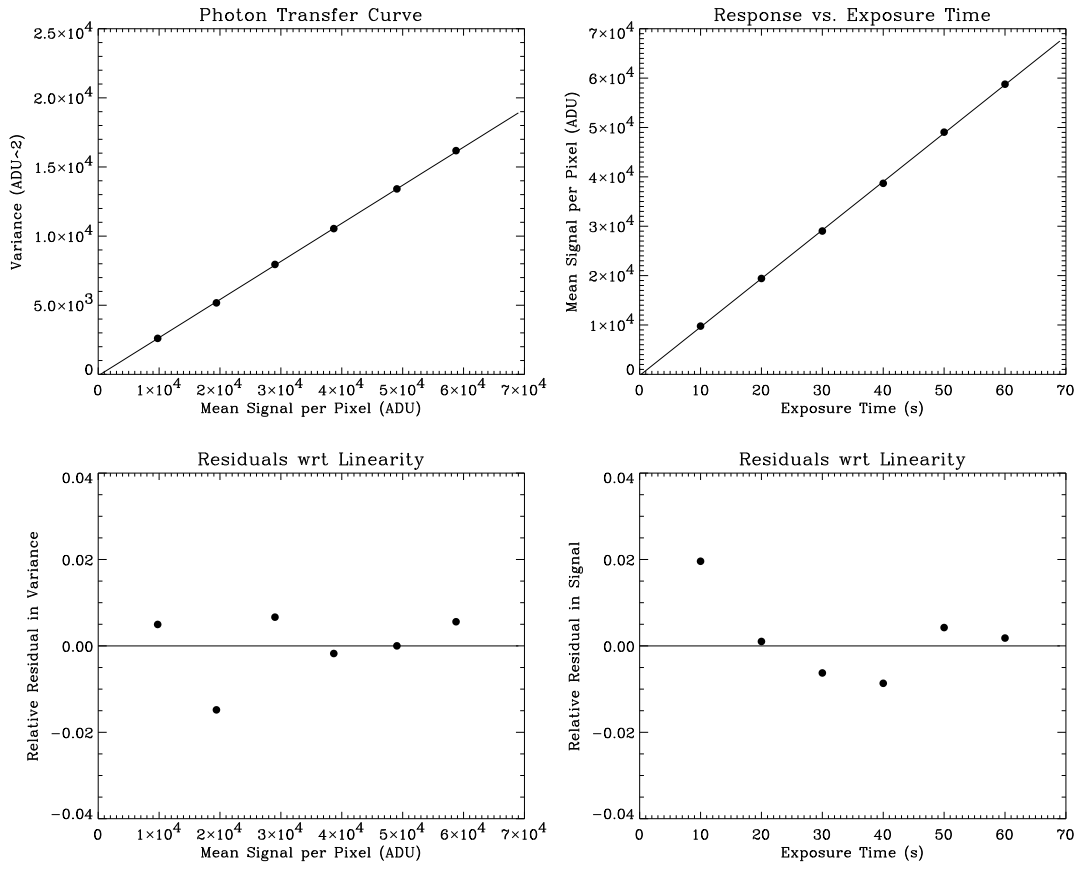


Fig. 2.— Performance curves for the GENII Camera, Amplifier B, Gain Setting 1.0.

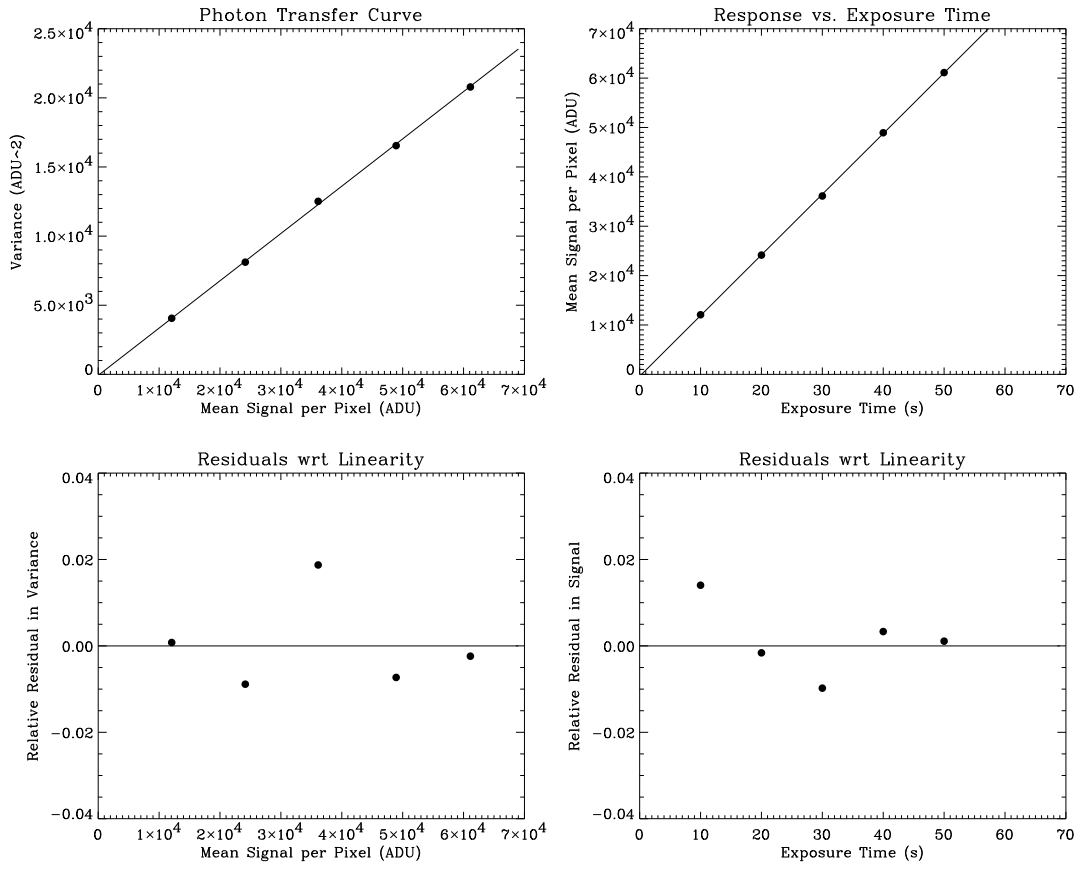


Fig. 3.— Performance curves for the GENII Camera, Amplifier C, Gain Setting 1.0.

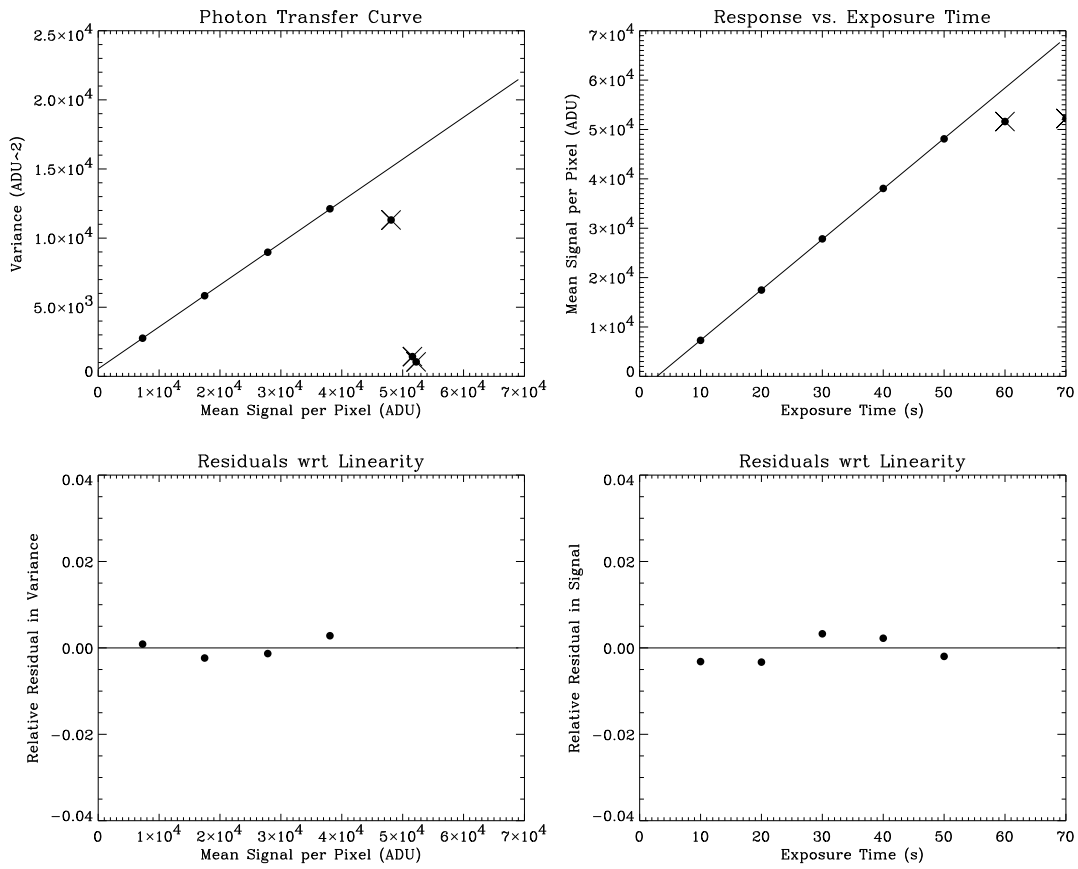


Fig. 4.— Performance curves for the GENII Camera, Amplifier D, Gain Setting 1.0.

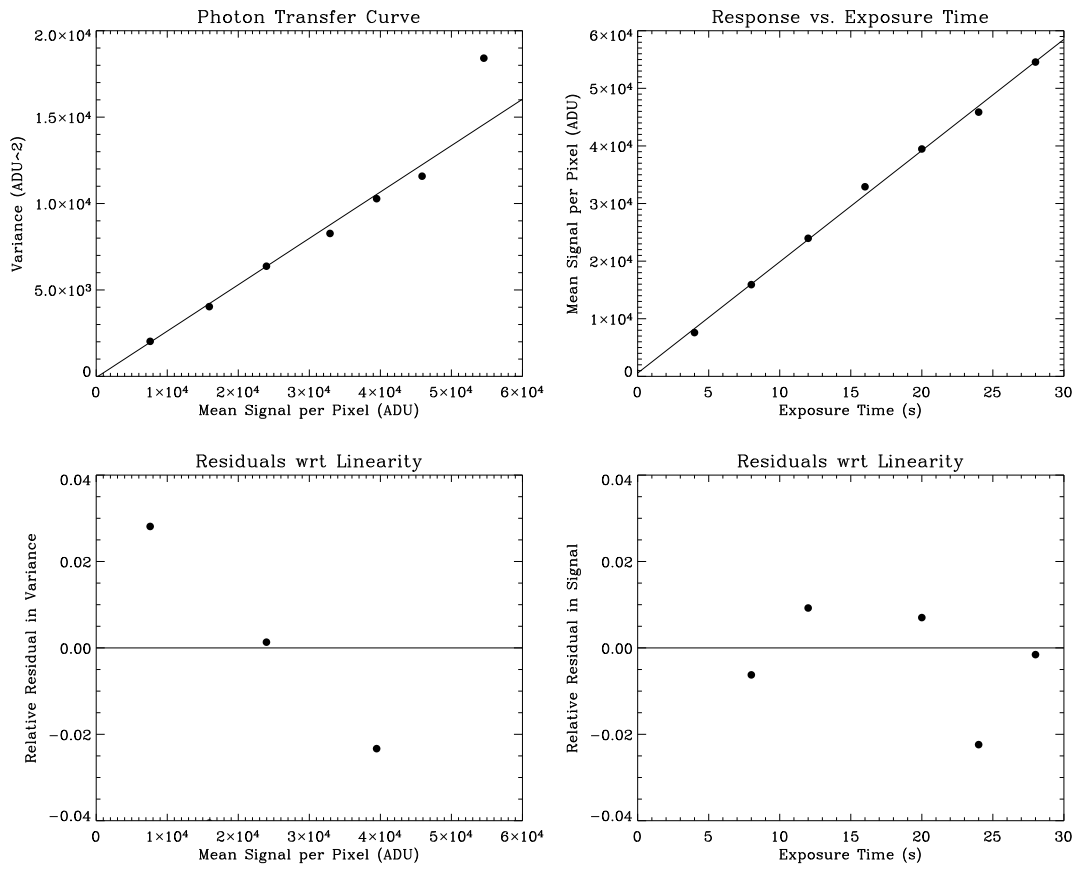


Fig. 5.— Performance curves for the GENI Camera, LOW gain, Trial 1.

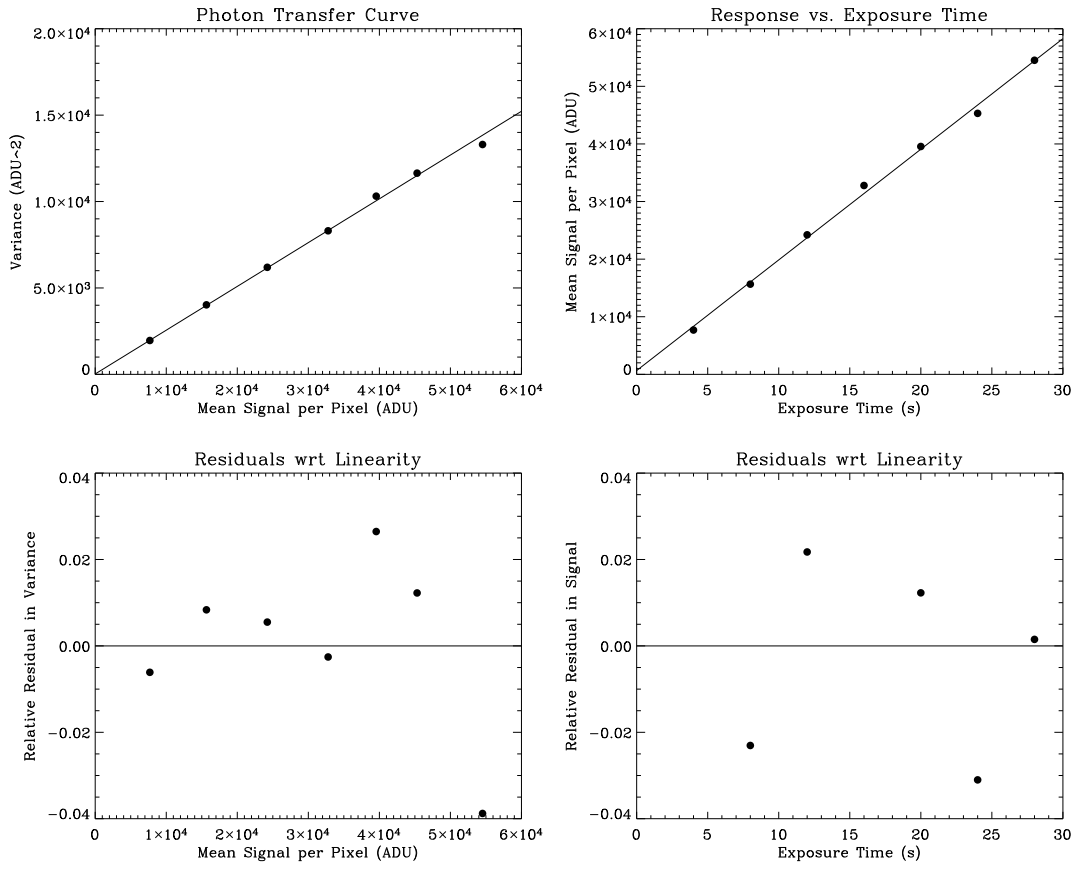


Fig. 6.— Performance curves for the GENI Camera, LOW gain, Trial 2.

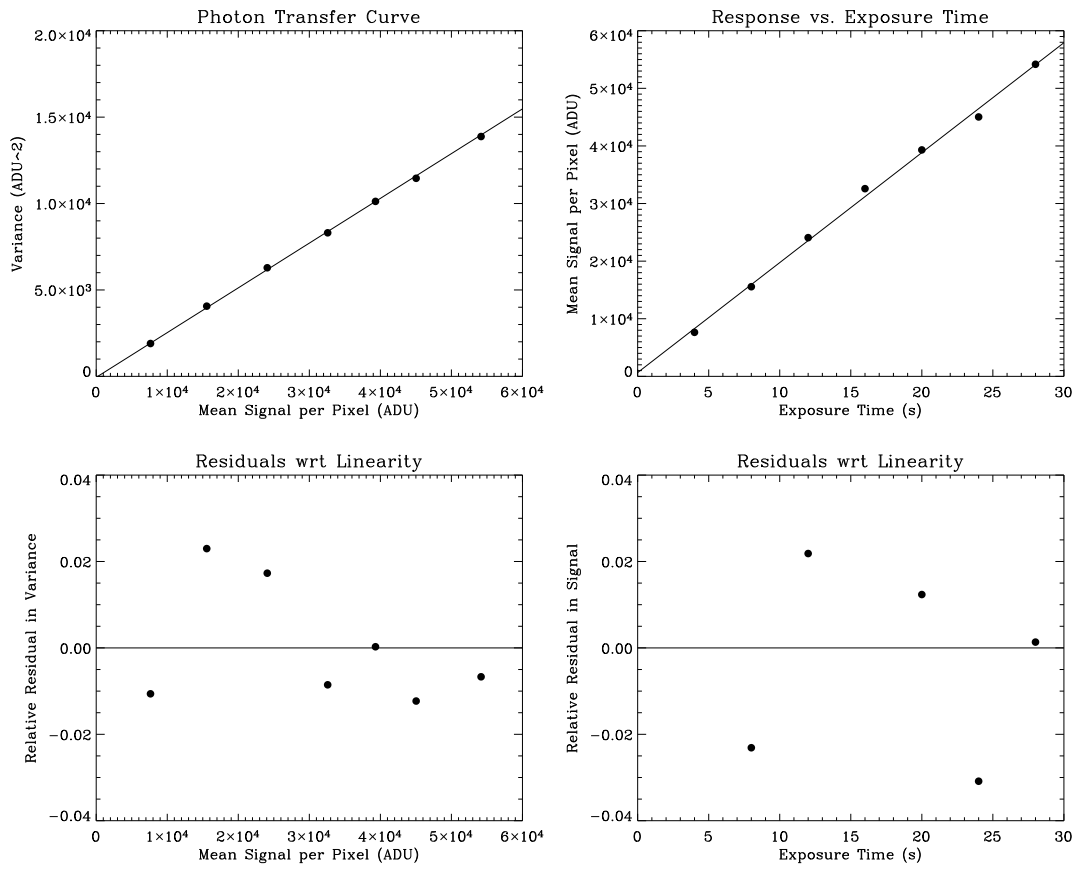


Fig. 7.— Performance curves for the GENI Camera, LOW gain, Trial 3.

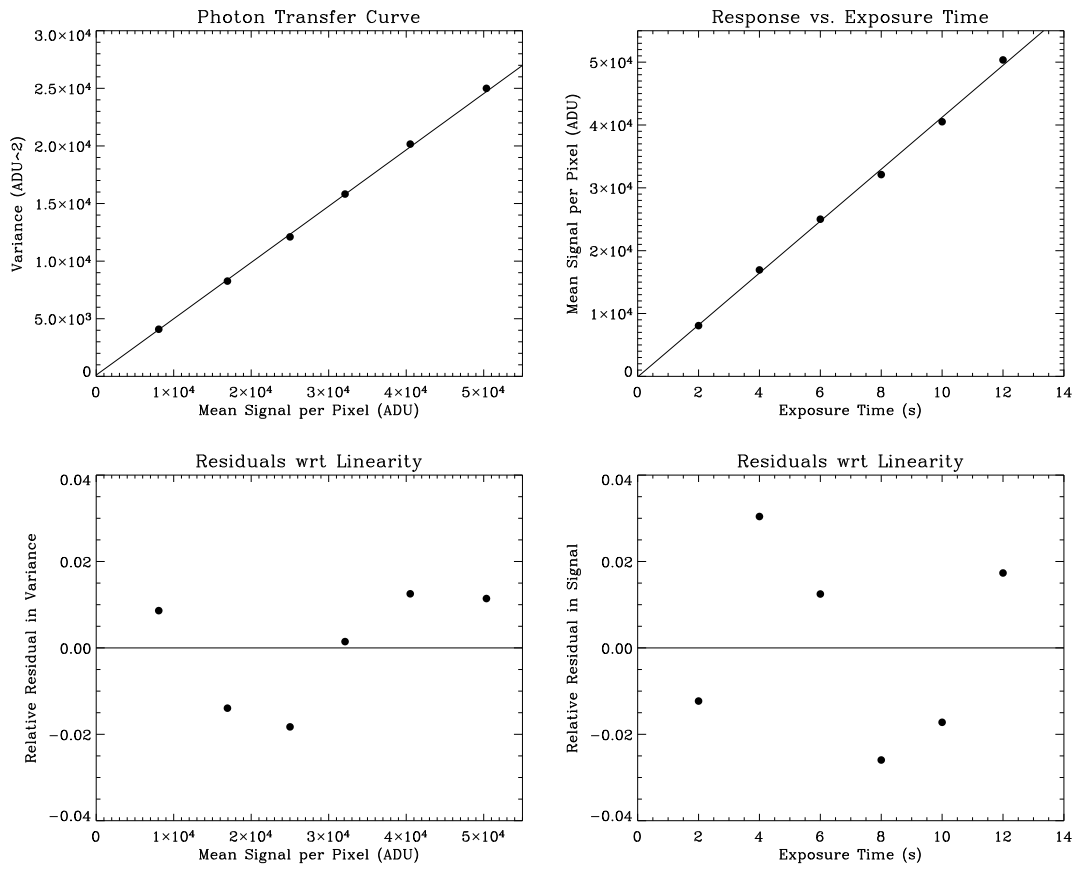


Fig. 8.— Performance curves for the GENI Camera, HIGH gain, Trial 1.

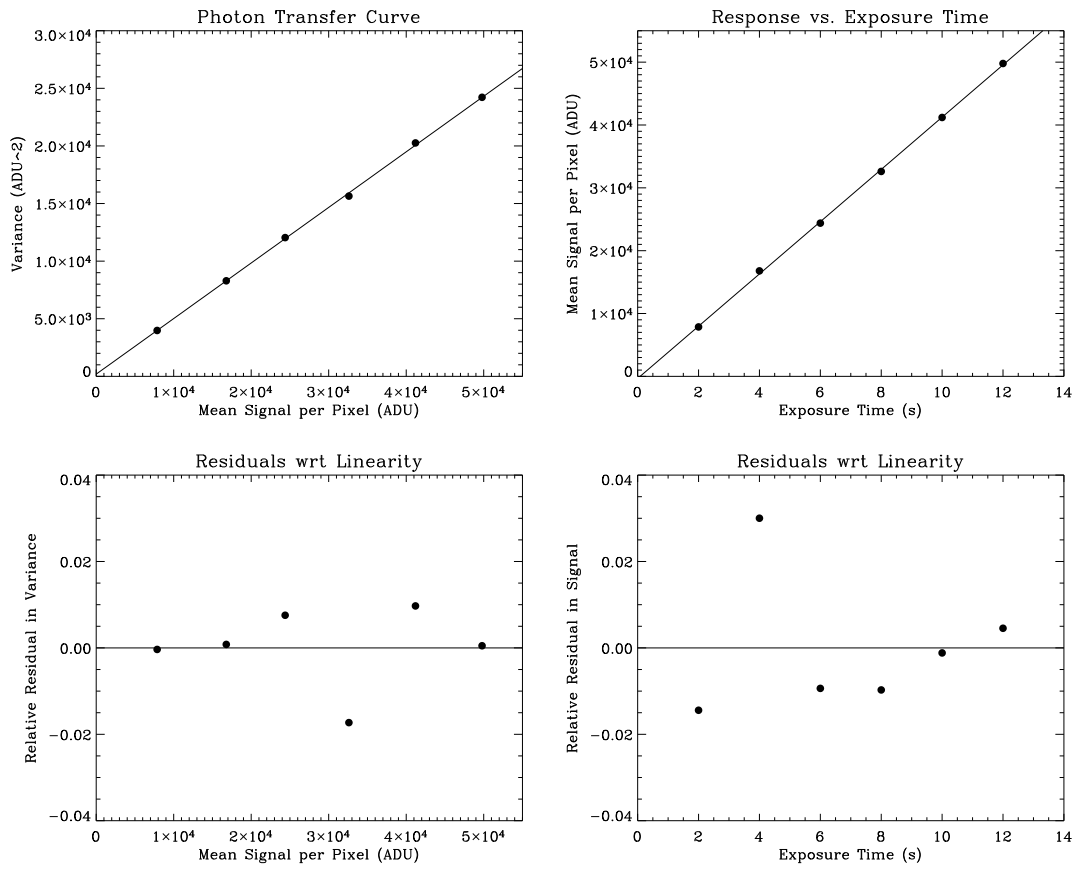


Fig. 9.— Performance curves for the GENI Camera, HIGH gain, Trial 2.

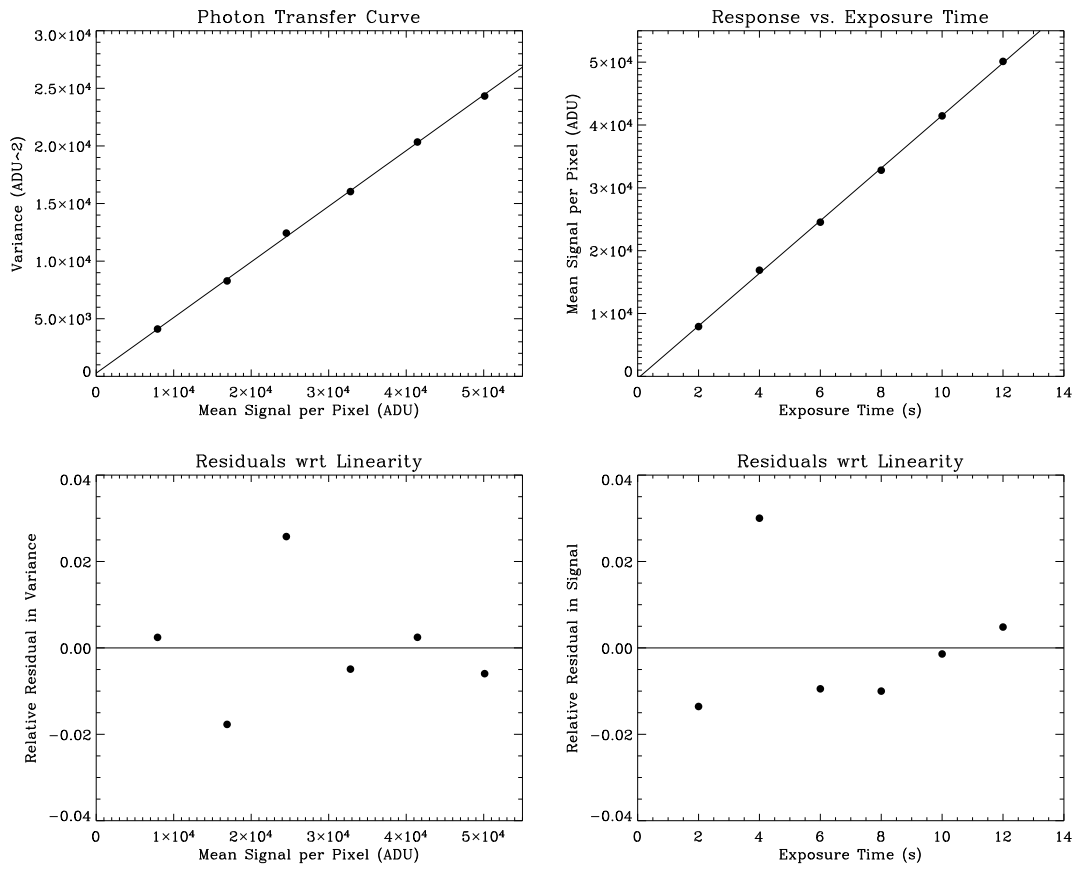


Fig. 10.— Performance curves for the GENI Camera, HIGH gain, Trial 3.